

## Dynamics of solitons and polarons in the quasi-one-dimensional $MX$ chain compound $[\text{Pt}(\text{en})_2][\text{Pt}(\text{en})_2\text{I}_2](\text{ClO}_4)_4$

H. Okamoto and Y. Oka

*Research Institute for Scientific Measurements, Tohoku University, Katahira, Sendai 980, Japan*

T. Mitani

*Japan Advanced Institute of Science and Technology, Ishikawa 923-12, Japan*

M. Yamashita

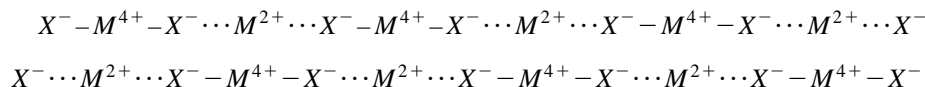
*Graduate School of Human Informatics, Nagoya University, Nagoya 464-01, Japan*

(Received 4 August 1995; revised manuscript received 20 May 1996)

The dynamics of solitons and polarons have been studied in a  $[\text{Pt}(\text{en})_2][\text{Pt}(\text{en})_2\text{I}_2](\text{ClO}_4)_4$  single crystal using photoinduced infrared absorption measurements. The annihilation process of the gap states is well explained by the bimolecular recombination model. Both carriers are long lived at low temperatures due to their finite pinning energies, and their decay characteristics are strongly temperature dependent. The temperature dependences of the rate constant of recombination for both carriers clearly show a crossover of the transport mechanism from hopping to tunneling with decrease of temperature. This behavior of the gap states is in contrast to that observed in transpolyacetylene. [S0163-1829(97)03709-0]

The remarkable tunability of the charge-density-wave (CDW) state in the halogen ( $X=\text{Cl}, \text{Br}, \text{I}$ )-bridged metal ( $M=\text{Ni}, \text{Pd}, \text{Pt}$ ) complex (or equivalently the  $MX$  chain compound), has made this a model material for the study of

the electron-lattice (e-l) and electron-electron interactions in the one-dimensional (1D) Peierls-Hubbard system.<sup>1-3</sup> Moreover, the broken symmetry degenerate ground states expressed as



lead to the prediction of spin solitons and charged solitons for the elementary excitations as well as polarons,<sup>4-6</sup> similarly to the conjugated polymers such as transpolyacetylene  $[(\text{CH})_x]$ .

Our previous measurements of photoinduced absorption (PA) on the  $MX$  chain compounds having different dimensionality of CDW ( $[\text{Pt}(\text{en})_2][\text{Pt}(\text{en})_2\text{X}_2](\text{ClO}_4)_4$  ( $\text{en}=\text{ethylenediamine}$ ) and  $[\text{Pt}(\text{chxn})_2][\text{Pt}(\text{chxn})_2\text{X}_2]\text{X}_4$  ( $\text{chxn}=\text{cyclohexanediamine}$ )) have demonstrated that the two types of gap state, namely, charged solitons and polarons are photogenerated.<sup>7,8</sup> In  $[\text{Pt}(\text{en})_2][\text{Pt}(\text{en})_2\text{X}_2](\text{ClO}_4)_4$  ( $X=\text{Br}, \text{I}$ ) where the interchain interaction of CDW is weak, the mid-gap band denoted as **b** is observed at almost half of the gap energies, which is attributable to charged solitons. In  $[\text{Pt}(\text{chxn})_2][\text{Pt}(\text{chxn})_2\text{X}_2]\text{X}_4$  ( $X=\text{Br}, \text{I}$ ) having two dimensionally ordered CDW, photogeneration of solitons is suppressed. Besides the midgap band **b**, there have been observed two PA bands **a**<sub>1</sub> and **a**<sub>2</sub> insensitive to the dimensionality of CDW, which are assigned to polarons. Spectral shapes of these PA signals due to charged solitons and polarons are found in agreement with those predicted by theoretical models.<sup>9-11</sup>

In the  $MX$  chain compounds, the dynamical behaviors of the gap states are considered to depend on the magnitude of the e-l interaction.<sup>3,8</sup> It has been found in the  $X=\text{Cl}$  compound,  $[\text{Pt}(\text{en})_2][\text{Pt}(\text{en})_2\text{Cl}_2](\text{ClO}_4)_4$ , that the exciton luminescence shows large Stokes shift ( $\sim 1.5$  eV),<sup>1</sup> and the photoinduced absorption due to the gap state does not decay at 77 K.<sup>12</sup> These phenomena demonstrate the strong effect of the e-l interaction on the photoexcited states. By changing the bridging halogen ion  $X$  from Cl to I, the displacements of  $X$  from the midpoints between the neighboring metal ions decrease<sup>1,3</sup> and, therefore, the effect of the e-l interaction will relatively decrease.<sup>3,7</sup> In the  $X=\text{I}$  compound,  $[\text{Pt}(\text{en})_2][\text{Pt}(\text{en})_2\text{I}_2](\text{ClO}_4)_4$ , however, the Stokes shift of luminescence is still large ( $\sim 0.8$  eV),<sup>1</sup> and the lifetime of the photoinduced gap states is more than a minute at 77 K.<sup>7</sup> These results suggest that the e-l interaction might also play an important role in the dynamics of the photoexcited states even in the  $X=\text{I}$  compound.

In this paper, we report the dynamics of the gap states in the  $[\text{Pt}(\text{en})_2][\text{Pt}(\text{en})_2\text{I}_2](\text{ClO}_4)_4$  compound on the basis of the excitation-power, time, and temperature dependences of the PA signals. (Hereafter, this complex is expressed by Pt-I.)

Our attention is focused especially on the transport mechanism of the photoinduced gap states. The excitation-power and time dependences of the PA signals could be explained by the simple bimolecular recombination model, and the intensity and the decay rate of the PA signals are found to be strongly dependent on temperature. From the analysis of the results in the framework of the bimolecular recombination model, we propose two types of transport mechanism, hopping and tunneling, for both charged solitons and polarons, depending on temperature. These two mechanisms are well interpreted by taking into account the e-I interactions and the quantum lattice fluctuations. Moreover, the origin of the photoconductivity will be discussed by comparing the activation energy of the photoconductivity with that of the recombination rate for photoproducts, which can be derived from the temperature dependence of the PA signals.

The PA measurements were made by using a Fourier-transform infrared spectrometer (Nicolet system 800) equipped with an InSb detector. The experimental procedures to obtain PA spectra have been reported in detail elsewhere.<sup>13</sup> Photoconductivities were measured by the two-probe method with the usual lock-in technique. As the excitation light, Ar laser (5145 Å) was used for the measurements of both PA spectra and photoconductivities. The single crystal was synthesized in the same way as reported in Ref. 3 and mounted on the cold finger of an Air Products cryostat allowing control of the sample temperature between 300 and 10 K.

The PA spectrum  $\Delta\alpha$  [photoinduced change of  $\alpha(=\tilde{k}d)$ ] of the Pt-I single crystal at 77 K was presented in Fig. 1(a). Here,  $\tilde{k}$  and  $d$  are the absorption coefficient and the thickness of the sample, respectively. In the measurements, the power of the excitation lights was 5 mW/cm<sup>2</sup>, and both the excitation lights and the transmission lights are polarized parallel to the chain axis  $b$ . As previously reported in Ref. 7, the structure  $\mathbf{a}_1$  and  $\mathbf{a}_2$  are assigned to polarons and the mid-gap structure  $\mathbf{b}$  to charged solitons. By adding the three Gaussian bands shown in Fig. 1(b), the obtained PA spectrum is well reproduced as the dotted line in Fig. 1(a). As theoretically demonstrated,<sup>11</sup> absorption for solitons or polarons in the  $MX$  chain compounds has generally a Gaussian spectral shape because of the fluctuation of lattice, namely the zero-point oscillation of bridging halogen ions.

Firstly, we discuss the annihilation process of the photo-products. As for this, the excitation-power dependence and the time characteristics of the PA signals give important information. In Fig. 2 the integrated intensities of the PA signals  $I_{PA}$  are plotted as a function of the excitation power  $I_{ex}$  at 77 K (open marks) and 130 K (solid marks). The data of  $I_{PA}$  are almost proportional to the square root of  $I_{ex}$  at both temperatures, as drawn by the dotted lines (77 K) and the broken lines (130 K), suggesting a bimolecular recombination of photocarriers. When neglecting the interaction between polarons and charged solitons, the bimolecular recombination process is simply expressed by a phenomenological rate equation,

$$dN_p/dt = \Phi_p I - k_p N_p^2, \quad (1a)$$

$$dN_s/dt = \Phi_s I - k_s N_s^2, \quad (1b)$$

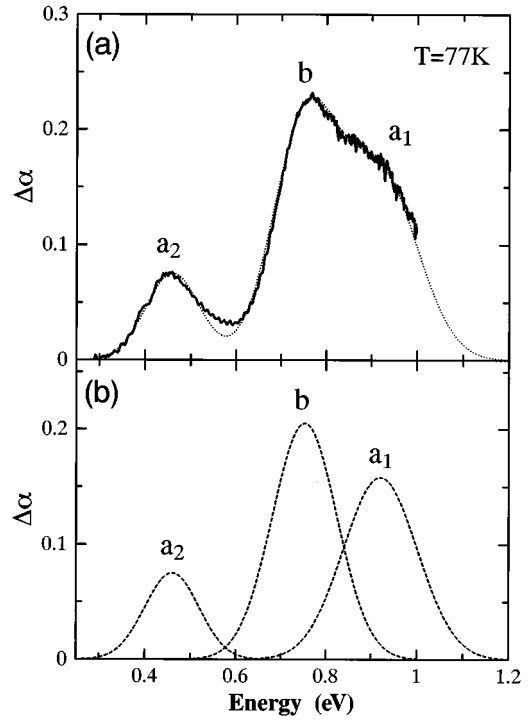


FIG. 1. The photoinduced absorption spectrum at 77 K [solid line in (a)]. Both the transmission light and the excitation light (5145 Å) are polarized parallel to the chain axis  $b$ . Dotted line in (a) is the sum of the three Gaussian spectra shown by the broken lines in (b).

where  $N$  is the number of polarons or solitons per unit volume,  $I$  is the photon number of excitation light per unit volume ( $I \propto I_{ex}$ ),  $\Phi$  is the generation efficiency of photocarriers,  $k$  is the rate constant of recombination. The  $p$  and  $s$  denote

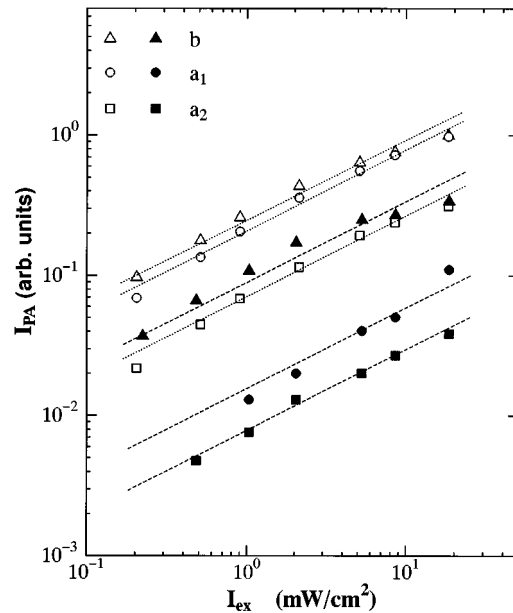


FIG. 2. The integrated intensities  $I_{PA}$  of the PA bands  $\mathbf{a}_1$  (circles),  $\mathbf{a}_2$  (rectangles), and  $\mathbf{b}$  (triangles) as a function of the excitation power  $I_{ex}$  at 77 K (open marks) and 130 K (solid marks). The dotted lines and the broken lines denote  $I_{PA} \propto I_{ex}^{0.5}$ .

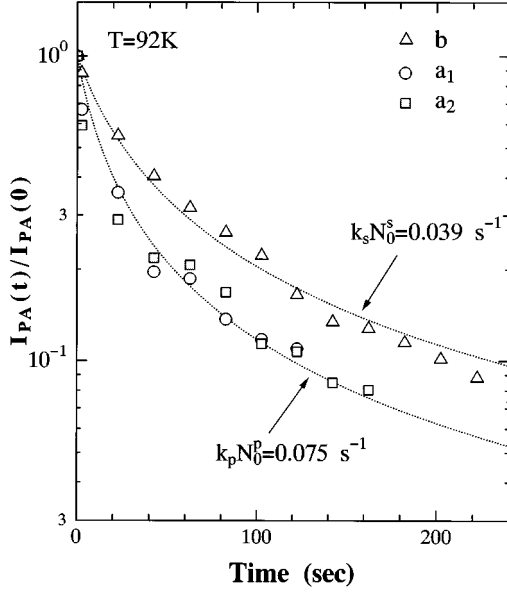


FIG. 3. Time dependences of the normalized intensities of the PA signals at 92 K. The dotted lines show the Eq. (2) for the indicated values of  $k_s N_0^s$  and  $k_p N_0^p$ .

polarens and charge solitons, respectively. The number of carriers in the steady state  $N_0$  ( $N_0^p$  for polarens and  $N_0^s$  for charged solitons) is expressed as  $(\Phi_{s,p} I / k_{s,p})^{0.5}$ . The square-root dependence of  $N_0^{s,p}$  on  $I$  agrees with the observed dependence of  $I_{PA}$  on  $I_{ex}$ . The time dependence of  $N_{s,p}$  is expressed as the following simple formula:

$$N_p(t)/N_0^p = (1 + k_p N_0^p t)^{-1}, \quad (2a)$$

$$N_s(t)/N_0^s = (1 + k_s N_0^s t)^{-1}. \quad (2b)$$

In Fig. 3, time dependences of the normalized intensities of the PA signals at 92 K are plotted in logarithmic scale. The charged solitons detected as the **b** band are found to be longer lived than the polarens detected as the **a<sub>1</sub>** and **a<sub>2</sub>** bands. The time characteristics of the PA signals can be well reproduced by the broken lines using Eqs. (2a) and (2b) with the parameters  $k_s N_0^s$  for charged solitons and  $k_p N_0^p$  for polarens given in Fig. 3. This also demonstrates that the bimolecular recombination model expressed by Eqs. (1a) and (1b) is appropriate for both charged solitons and polarens in the Pt-I complex.

The next problem is to clarify the transport mechanism of photocarriers. In the bimolecular recombination model discussed here,  $k_{s,p}$  is determined by the encounter rate for photocarriers,<sup>14</sup> so that  $k_s$  and  $k_p$  are proportional to the mobilities,  $\mu_s$  for charged solitons and  $\mu_p$  for polarens, respectively.<sup>15</sup> Therefore, important information about the transport mechanism of charged solitons and polarens will be obtained from the temperature dependence of  $k_s$  and  $k_p$ . In order to evaluate their temperature dependence, we measured the PA spectra in the steady state and their time characteristics at various temperatures. As mentioned above,  $N_0^{s,p} = (\Phi_{s,p} I / k_{s,p})^{0.5}$ , according to the bimolecular recombination model, so that temperature dependence of  $(N_0^{s,p})^{-2}$  or equivalently  $I_{PA}^{-2}$  reflects the temperature dependence of

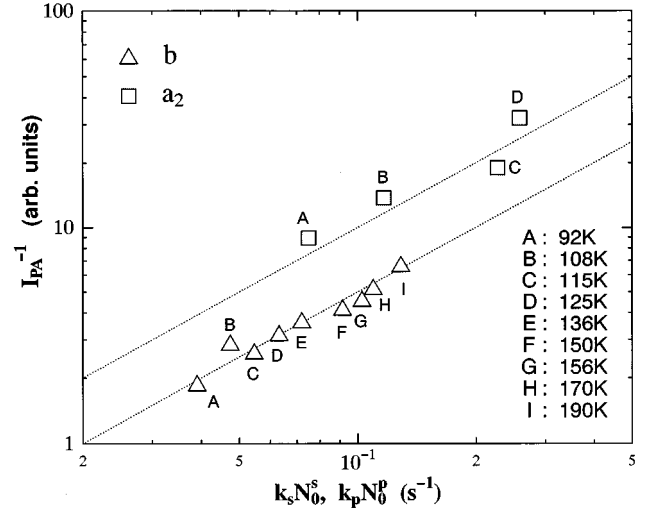


FIG. 4. Relation between  $I_{PA}^{-1}$  and  $k_{s,p} N_0^{s,p}$ . The dotted lines indicate  $I_{PA}^{-1} \propto k_s N_0^s$  and  $k_p N_0^p$ .

$k_{s,p}$ , if the generation efficiency of photocarriers  $\Phi_{s,p}$  is independent of temperature. The linear relation between  $k_{s,p}$  and  $I_{PA}^{-2}$  can be examined by evaluating the  $k_{s,p}$  values at various temperatures. As shown in Fig. 3,  $k_s N_0^s$  and  $k_p N_0^p$  are the fitting parameters to reproduce the time dependences of the PA intensities. Therefore, we displayed the relation between  $k_{s,p} N_0^{s,p} (\propto k_{s,p} I_{PA})$  and  $I_{PA}^{-1}$  in Fig. 4 for **b** and **a<sub>2</sub>** bands at several temperatures. With increase of temperature, the values of both  $k_s N_0^s$  and  $k_p N_0^p$  increase showing that the decay of PA signals becomes fast. As clearly seen in Fig. 4,  $I_{PA}^{-1}$  is proportional to  $k N_0$  for both carriers, that is,  $k$  is proportional to  $I_{PA}^{-2}$ . This linear relation also demonstrates that the temperature dependences of the generation efficiency of carriers,  $\Phi_s$  for charged solitons and  $\Phi_p$  for polarens, are negligible as compared with those of  $k_s$  and  $k_p$ , respectively. If  $\Phi_{s,p}$  was strongly temperature dependent, the temperature dependence of  $I_{PA}^{-1} (\propto [k_{s,p}(T) / \Phi_{s,p}(T)]^{0.5})$  should not be equal to that of  $k_{s,p} N_{0s,p} (\propto [k_{s,p}(T) \cdot \Phi_{s,p}(T)]^{0.5})$ .

Figure 5 is the Arrhenius plot of  $[I_{PA}(T) / I_{PA}(77 \text{ K})]^{-2}$  for **a<sub>1,2</sub>** and **b** bands, which shows the temperature dependence of  $k_p$  for polarens and  $k_s$  for charged solitons, respectively. In the temperature regions above 120 K for polarens and above 200 K for charged solitons, the intensity of the PA signals remarkably decreases with increase of temperature. As seen in Fig. 5,  $[I_{PA}(T) / I_{PA}(77 \text{ K})]^{-2}$  in these high-temperature regions almost follows the activation-type formula  $[\exp(-\Delta/kT)]$  as plotted by the dotted lines. The values of  $\Delta$ ,  $0.76 \pm 0.1$  eV for charged solitons and  $0.28 \pm 0.04$  eV for polarens, correspond to the activation energy of  $\mu_s$  and  $\mu_p$ , respectively. Namely, the carriers are strongly bound to the lattice due to the e-l interaction and a hopping mechanism dominates the transport properties of both charged solitons and polarens in the higher temperature region.

At lower temperatures, i.e.,  $T < 120$  K for polarens and  $T < 200$  K for charged solitons, a different mechanism should be considered for carrier transport, since the temperature dependences of  $[I_{PA}(T) / I_{PA}(77 \text{ K})]^{-2}$  (or  $\mu_s$  and  $\mu_p$ ) are

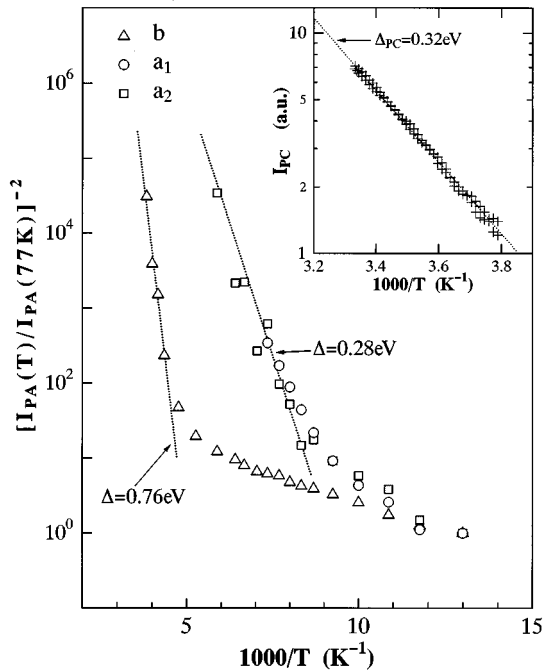


FIG. 5. Temperature dependences of the normalized intensities of the PA signals  $[I_{PA}(T)/I_{PA}(77\text{ K})]^{-2}$ . Inset is temperature dependence of the photoconductivity along the chain axis  $b$  with the excitation light (5145 Å) polarized parallel to  $b$ .

rather small. A reasonable interpretation for the transport mechanism in these low-temperature regions is a tunneling process. The vibration relating to the transport processes of polarons and charged solitons is the stretching mode of the bridging iodine ions. According to the Raman measurements, the frequency of the symmetric stretching mode of the bridging iodine ions  $h\nu_s$  is  $\sim 130\text{ cm}^{-1}$ .<sup>16</sup> The temperature of the zero-point oscillation  $T_0 = h\nu_s/2$  is, therefore, 90 K. As seen in Fig. 5, the critical temperature  $T_c$  where the transport mechanism changes, is  $\sim 115\text{ K}$  for polarons, which is close to  $T_0$  (90 K). It is quite natural that a crossover from a classical hopping process to a quantum-tunneling process occurs with decrease of temperature. For charged solitons, the critical temperature  $T_c \sim 200\text{ K}$  is considerably larger than  $T_0$ , so that a phonon-assisted tunneling process might be dominant for the transport.

Let us go to the discussion about the origin of the photoconductivities in the Pt-I complex. In the inset of Fig. 5, the photocurrent  $I_{PC}$  along the chain axis  $b$  with the excitation light polarized parallel to  $b$ , is plotted as a function of temperature. In the measurements, we adjusted the intensity of the excitation light  $I_{ex}$  and the magnitude of the external electric field  $F$  so that  $I_{PC}$  is proportional to  $I_{ex}$  and  $F$ . The temperature dependence of  $I_{PC}$  in Fig. 5 is in agreement with that reported by Haruki, Tananka, and Kurita.<sup>17</sup> The activation energy of photocurrent  $\Delta_{PC}$  is estimated about 0.32 eV in the temperature region from 300 to 260 K, below which photocurrent could not be detected because of the limitation of the sensitivity. This value (0.32 eV) is almost equal to the activation energy of  $k_p$  or  $\mu_p$  ( $0.28 \pm 0.04\text{ eV}$ ) for polarons obtained from the PA measurements. This suggests that polarons will be responsible for the photoconductivities.

If the oscillator strengths of the transitions due to the gap

states ( $f_s$  for a charged soliton and  $f_p$  for a polaron) are known, the parameter values of  $N_0^s$  and  $N_0^p$  can be evaluated by using the integrated intensity of the photoinduced absorption bands. The magnitudes of  $f_s$  and  $f_p$  have not been obtained experimentally, so that we will use the theoretical evaluations for them. According to the theoretical calculation by Iwano and Nasu,<sup>11</sup> both  $f_s$  and  $f_p$  (the sum of the strength of the  $a_1$  and  $a_2$  bands) are almost equal to  $2.8 \times f_{CT}$ .  $f_{CT}$  is the oscillator strength of the intermetallic charge-transfer (CT) band for a unit of  $[M^{4+} - X^- - M^{2+} - X^-]$ . Here, we introduce the following relation:

$$2N_0^{s,p}f_{s,p} = (m_0c\sqrt{\epsilon_b})/(2\pi^2e^2) \int \{\alpha_{s,p}(\omega)/d_s\}d\omega, \quad (3)$$

where  $\epsilon_b$  is the dielectric constant in the gap region and  $d_s$  is the absorption depth for the excitation light, which is the inverse of the absorption coefficient. The factor 2 in the left-hand side comes from the fact that an electron polaron and a hole polaron (or a negatively charged soliton and a positively charged soliton) give the same absorption spectrum.  $d_s$ ,  $\epsilon_b$ , and  $f_{CT}$  can be obtained from the analysis of the polarized reflectivity spectrum by utilizing the Kramers-Kronig transformation.<sup>18</sup> Using that  $d_s = 2.7 \times 10^{-6}\text{ cm}^{-1}$ ,  $\epsilon_b = 10$ ,  $f_{CT} = 6$ ,<sup>18</sup> and  $\alpha_{s,p}$  experimentally obtained, Eq. (3) yields that  $N_0^s = 8.6 \times 10^{18}\text{ cm}^{-3}$  and  $N_0^p = 6.9 \times 10^{18}\text{ cm}^{-3}$  at 92 K. Using the values of  $k_{s,p}N_0^{s,p}$  given in Fig. 3, we obtained the values of the rate constant at 92 K as  $k_s = 4.5 \times 10^{-21}\text{ cm}^3\text{ s}^{-1}$  and  $k_p = 1.1 \times 10^{-20}\text{ cm}^3\text{ s}^{-1}$ . The generation efficiencies were calculated from the relation  $N_0 = (\Phi I/k)^{0.5}$  as  $\Phi_s = 7.0 \times 10^{-5}$  and  $\Phi_p = 1.1 \times 10^{-4}$ . In this estimation, the loss of the excitation light ( $\sim 40\%$ ) due to the reflection was taken into account.

As previously reported, the PA signals for charged solitons and polarons are strongly dependent on the excitation energies  $E_{ex}$ .<sup>7</sup> The excitation of the CT exciton does not contribute to the generation of charged solitons and polarons. This can be attributed to the excitonic effect on the photoexcited electron-hole pairs. With an increase of  $E_{ex}$ , both  $\Phi_s$  and  $\Phi_p$  considerably increase and show maxima around 3.2 eV.<sup>19</sup> Using the energy dependences of the PA signals and the absorption coefficients,  $\Phi_{s,p}$  for  $E_{ex} = 3.2\text{ eV}$  are estimated as  $\Phi_s = 5.0 \times 10^{-4}$  and  $\Phi_p = 1.7 \times 10^{-3}$ .

Finally, we note the difference of the dynamical properties of charged solitons and polarons between trans-(CH)<sub>x</sub> (Ref. 20) and the MX compound. In trans-(CH)<sub>x</sub>, the transfer energy  $T$  is much larger than the e-l interaction energy. In this case, charged solitons and polarons are not self-trapped but move freely along the chain, and the interactions of the gap states with phonons determine their diffusion constants.<sup>21,22</sup> In fact, the PA signals due to charged solitons generated in a single chain decay in subpicosecond time scales by geminate recombinations, and those due to polarons decay within several tenths of psec by encountering neutral solitons even at low temperatures.<sup>23</sup> On the other hand, in the MX compound, the e-l interaction  $S$  is comparable to  $T$ ,<sup>9-11</sup> so that solitons and polarons are localized with the finite pinning energies. In fact, when changing the bridging halogen ion from I to Cl, the effect of the e-l interaction increases and the decay of the PA signals has been

found to become slower.<sup>24</sup> This is due to the increase of the potential barrier for transport of carriers induced by the increase of  $S/T$ .

In summary, both charged solitons and polarons are long lived in the Pt-I complex, suggesting their finite pinning energies. The temperature dependences of the rate constant for the bimolecular recombination,  $k_s$  for charged solitons and  $k_p$  for polarons derived from the PA measurements, clearly show the crossover of the transport mechanism from the classical hopping process to the quantum tunneling process for both carriers. These behaviors of the gap states in the Pt-I

complex are in contrast with those in trans-(CH)<sub>x</sub>. Finally, we emphasize again that the PA measurements presented in this paper directly detect the dynamical behaviors of charged solitons and polarons, and enable us to study systematically transport properties of photocarriers in the 1D electron-lattice coupling systems.

The authors wish to thank Dr. Iwano and Professor Nasu (KEK) for many enlightening discussions. This work was partly supported by a Grant-in-Aid from the Ministry of Education, Science, and Culture, Japan.

- 
- <sup>1</sup>Y. Wada, T. Mitani, M. Yamashita, and T. Koda, *J. Phys. Soc. Jpn.* **54**, 3143 (1985).
- <sup>2</sup>H. Okamoto, K. Torumi, T. Mitani, and M. Yamashita, *Phys. Rev. B* **42**, 10 381 (1990).
- <sup>3</sup>H. Okamoto, T. Mitani, K. Toriumi, and M. Yamashita, *Mater. Sci. Eng. B* **13**, L9 (1992).
- <sup>4</sup>S. Ichinose, *Solid State Commun.* **50**, 137 (1984).
- <sup>5</sup>Y. Onodera, *J. Phys. Soc. Jpn.* **56**, 250 (1987).
- <sup>6</sup>D. Baeriswyl and A. R. Bishop, *J. Phys. C* **21**, 339 (1988).
- <sup>7</sup>H. Okamoto, T. Mitani, K. Toriumi, and M. Yamashita, *Phys. Rev. Lett.* **69**, 2248 (1992).
- <sup>8</sup>H. Okamoto and T. Mitani, *Prog. Theor. Phys.* **113**, 191 (1993).
- <sup>9</sup>J. T. Gammel, A. Saxena, I. Batistic, A. R. Bishop, and S. R. Phillpot, *Phys. Rev. B* **45**, 6408 (1992).
- <sup>10</sup>S. M. Weber-Milbrodt, J. T. Gammel, A. R. Bishop, and E. Y. Loh, Jr., *Phys. Rev. B* **45**, 6435 (1992).
- <sup>11</sup>K. Iwano and K. Nasu, *J. Phys. Soc. Jpn.* **61**, 1380 (1992).
- <sup>12</sup>S. Kurita, M. Haruki, and K. Miyagawa, *J. Phys. Soc. Jpn.* **57**, 1789 (1988).
- <sup>13</sup>H. Okamoto, K. Okaniwa, T. Mitani, K. Toriumi, and M. Yamashita, *Solid State Commun.* **77**, 465 (1991).
- <sup>14</sup>R. C. Powell and Z. G. Soos, *J. Lumin.* **11**, 1 (1975).
- <sup>15</sup>M. Pope and C. E. Swenberg, *Electronic Processes in Organic Crystals* (Oxford University Press, Oxford, 1982), p. 456.
- <sup>16</sup>R. J. H. Clark and M. Kurmoo, *J. Chem. Soc. Faraday Trans. 2* **79**, 519 (1983).
- <sup>17</sup>M. Haruki, M. Tanaka, and S. Kurita, *Synth. Met.* **19**, 901 (1987).
- <sup>18</sup>We measured the polarized reflectivity spectrum on the Pt-I single crystal with the electric vector parallel to the chain axis *b*. Our result is essentially the same as that reported by Wada *et al.* in Ref. 1. We used our result to obtain the optical constants and the related parameters ( $d_s$  and  $f_{CT}$ ).
- <sup>19</sup>H. Okamoto *et al.* (unpublished).
- <sup>20</sup>For a review, see A. J. Heeger, S. Kivelson, and J. R. Schrieffer, *Rev. Mod. Phys.* **60**, 781 (1988).
- <sup>21</sup>Y. Wada and J. R. Schrieffer, *Phys. Rev. B* **18**, 3897 (1978).
- <sup>22</sup>A. Terai and Y. Ono, *J. Phys. Soc. Jpn.* **55**, 213 (1986).
- <sup>23</sup>L. Rothberg, T. M. Jedju, S. Etemad, and G. L. Baker, *Phys. Rev. B* **36**, 7529 (1987).
- <sup>24</sup>H. Okamoto, Y. Oka, T. Mitani, K. Toriumi, and M. Yamashita, *Mol. Cryst. Liq. Cryst.* **256**, 161 (1994).